

Microstrip Transmission Line with Finite-Width Dielectric

CHARLES E. SMITH, MEMBER, IEEE, AND RAY-SUN CHANG, MEMBER, IEEE

Abstract—The results of a numerical solution for open microstrip transmission line with finite-width dielectric are presented for a quasi-TEM computational model. The related solution is based on moment methods using equivalent source models for the free and bound charges existing on boundary surfaces. Characteristic impedance and velocity of propagation are presented in graphical form for estimating the effects of dielectric truncation on microstrip circuits and for related circuit design.

INTRODUCTION

SINCE THE EARLY FIFTIES, microstrip transmission lines have received a great deal of attention from the electrical engineering community [1], [2]. The work in these areas has focused on the numerical solution of the infinite-width microstrip [3]–[5], rectangular sections of microstrip [6], [7], and the finite-width microstrip in a shielded box [8].¹ However, the characteristics of the practical case of the finite-width open microstrip transmission line, as shown in Fig. 1, have not been investigated and reported.

The purpose of this paper is to investigate the effects of truncation on open microstrip line with finite-width dielectrics. The results of this study are presented in the form of design diagrams. The case of truncated dielectric with infinite ground plane is considered because it approximates the practical case better than the idealized infinite-width model.

NUMERICAL SOLUTION

The microstrip problem of Fig. 1 has been solved using a free-space Green's function formulation in terms of equivalent charge sources coupled with a moment method solution [9]. This approach to electrostatic problems has been described by Harrington and Pontoppidan [10], by Adams and Mautz [8], [11], and, in a slightly different form, by Smith [12]. In this formulation, a set of coupled integral equations in terms of equivalent charges and a free-space Green's function are obtained by enforcing proper boundary conditions.

The quasi-static problem related to this analysis can be represented as two regions separated by a boundary C corresponding to the air-dielectric interface of the micro-

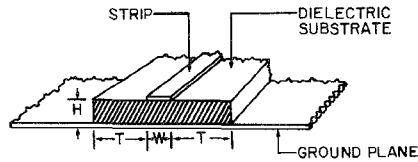


Fig. 1. Finite-width microstrip line with truncated dielectric substrate and infinite ground plane.

strip and its image [12]. The configuration reduces to a two-dimensional analysis of the microstrip cross section as shown in Fig. 1 or in the inserts of the other figures. In this case, the scalar (or Laplacian) potential for the exterior (Region 2) and interior (Region 1) areas can be represented in terms of sources on the boundary using the equivalence theorem [13]. The “equivalent” problem which consists of surface-type charge densities may be derived from Green's theorem applied to each region [10], [12]. Based on this approach, the scalar potential in either region can be expressed in terms of the equivalent sources as

$$\phi(\bar{\rho}) = \frac{1}{\epsilon_0} \int_C \sigma(\bar{\rho}') G_0(\bar{\rho}, \bar{\rho}') dC' \quad (1)$$

where $\sigma(\bar{\rho}')$ is the sum of the equivalent free and bound charge source densities on the interface, C is the interface contour boundary, $\bar{\rho}'$ and $\bar{\rho}$ are vector quantities representing the general source and field points, respectively, and the Green's function is

$$G_0(\bar{\rho}, \bar{\rho}') = \frac{1}{2\pi} \ln |\bar{\rho} - \bar{\rho}'|. \quad (2)$$

Under the assumption of a quasi-TEM model for this inhomogeneous structure, boundary conditions require continuity of the normal component of electric flux density, i.e., $\epsilon_1 E_{n1} = \epsilon_2 E_{n2}$, on the dielectric interface. Since $\bar{E} = -\nabla\phi$, it can be shown from (1) and this boundary condition, as applied in both regions, that

$$(\epsilon_r + 1) \frac{\sigma(\bar{\rho})}{2} + (\epsilon_r - 1) \oint_C \sigma(\bar{\rho}') \frac{\partial G_0(\bar{\rho}, \bar{\rho}')}{\partial n} dC' = 0 \quad (3)$$

where $\epsilon_r = \epsilon_2/\epsilon_1$, $\epsilon_1 = \epsilon_0$ (free-space permittivity), and the partial derivative is in respect to the outward normal to the interior region.

Equations (1) and (3) form a set of coupled integral equations in terms of the unknown charge density if the following boundary conditions for voltage V are enforced:

$$\phi(\bar{\rho}) = V \text{ on the strip}$$

Manuscript received February 26, 1979.

C. E. Smith is with the Electrical Engineering Department, University of Mississippi, University, MS 38677.

R. S. Chang is with Texas Instruments, Incorporated, Stafford, TX 77477.

¹A more detailed bibliography on recent work is presented in reference [8].

and

$$\phi(\rho) = -V \text{ on the strip image portions of the boundary} \quad (4)$$

where continuity of electric flux density on the dielectric interface has been insured by (3).

The solution of the related coupled integral equations ((1) and (3)) has been obtained with matrix or moment methods using pulse function expansion of the unknown equivalent sources and a "point-matching" or collocation technique [14].² Once the approximate solution for the total equivalent charge density is known from the moment method analysis, the free charge density ρ_c can be computed from the discontinuous nature of the electric flux density on a strip boundary where free charge exists. Thus it can be determined in a manner similar to that used for (3) that

$$\rho_c(\bar{\rho}) = D_{n1} - D_{n2} \\ = (\epsilon_r + 1) \frac{\sigma(\bar{\rho})}{2} + (\epsilon_r - 1) \int_C \sigma(\bar{\rho}') \frac{\partial G_0(\bar{\rho}, \bar{\rho}')}{\partial n} d\bar{c}. \quad (5)$$

Equation (5) can easily be expressed in terms of the known matrix coefficients and $\sigma(\bar{\rho})$ for subsequent analysis [10], [11]. Note that the approach is not limited to specific geometries, and arbitrary shaped inhomogeneous TEM transmission lines can be analyzed with this boundary-value problem approach [11]–[12].

RESULTS

A computer program based on this formulation has been developed to calculate a solution to this boundary-value problem. An attempt to validate this computer code has been made by computing the limiting case as the truncation width T approaches infinity with $W/H=2.0$ for the line of Fig. 1. A comparison of this computed data with previously reported results for the infinite-width microstrip is presented in Table I which indicates very good agreement between the different computations.

In addition, experimental measurements have been made on actual models of the finite-width microstrip for large ground plane widths W_p . In these experiments, the characteristic impedance was determined from time-domain reflectometry (TDR) measurements. Results are presented in Fig. 2 along with the computed data for specified finite-width lines. As can be seen, these TDR measurements do tend to indicate that the truncation of the dielectric does not influence the characteristic impedance for T/W ratios greater than one (for $\epsilon_r=4.7$). The small errors in these measurements can, for the most part, be attributed to inaccuracies in measurement of the relative dielectric constant of the microstrip board.

It might be expected that the characteristic impedance would not be highly dependent on dielectric width in this case because the fields are concentrated under the strip for these larger values of W/H and ϵ_r . The influence of the truncation is even more evident in the plot of the line charge density per unit width of Fig. 3. For a related

²The principal value of the integral of (3) was represented as a pulse expansion term of appropriate magnitude for moment method analysis.

TABLE I
COMPARISON OF CHARACTERISTIC IMPEDANCE OF FINITE-WIDTH AND
INFINITE-WIDTH MICROSTRIP TRANSMISSION LINE ($W/H=2.0$, $T/W=15.0$,
RELATIVE DIELECTRIC CONSTANT $\epsilon_r=16$)

Method	Z_0
Bryant and Weiss [3]	26.644 Ω
Farrar and Adams [4]	26.756 Ω
Smith [12]	26.879 Ω
Finite-width solution	26.783 Ω

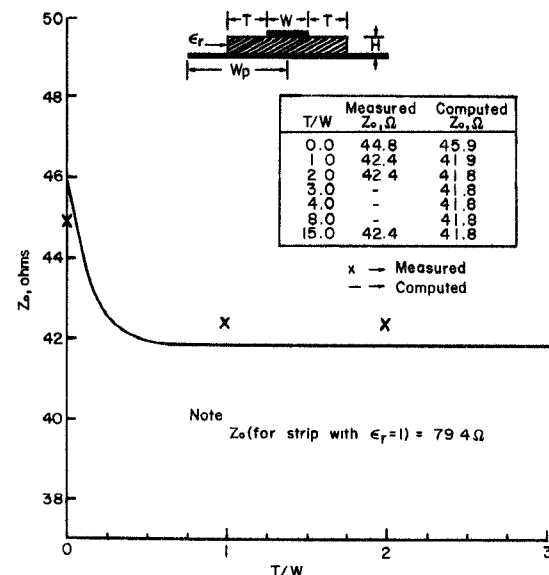


Fig. 2. Characteristic impedance for microstrip line ($W/H=2.47$, $\epsilon_r=4.7$, and $W_p/W > 15$).

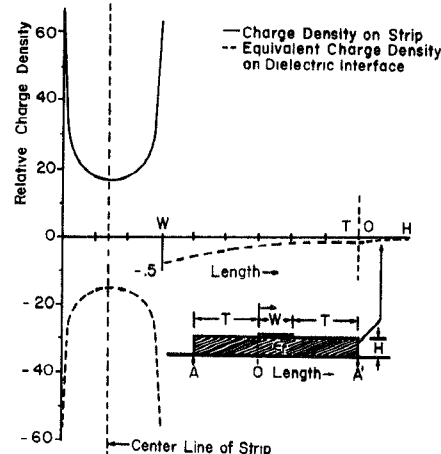
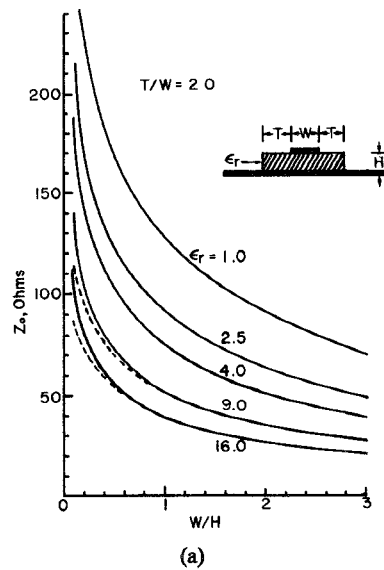
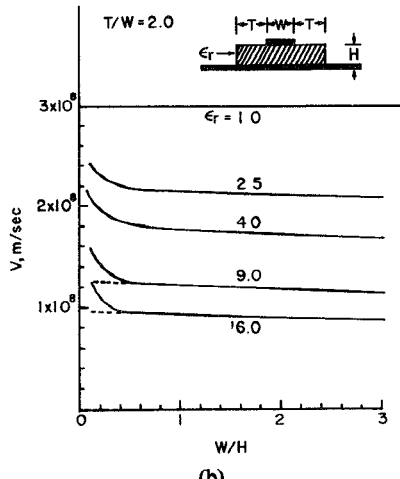


Fig. 3. Charge distribution on the strip and dielectric interface ($W/H=2$, $\epsilon_r=16$, and $T/W=2$).

infinite-width line, the equivalent line charge density on the dielectric interface decreases monotonically as a function of cross sectional length along the dielectric interface. In the truncated case of Fig. 3 ($T/W=2.0$), the equivalent charge has a discontinuity in slope at the edge of the dielectric. At this point, the charge density does indeed exhibit singular behavior as would be expected at an edge; but, this singular nature is not prominently evidenced in this plot because the magnitude of charge density is very small relative to that of the charge densities on, under,



(a)

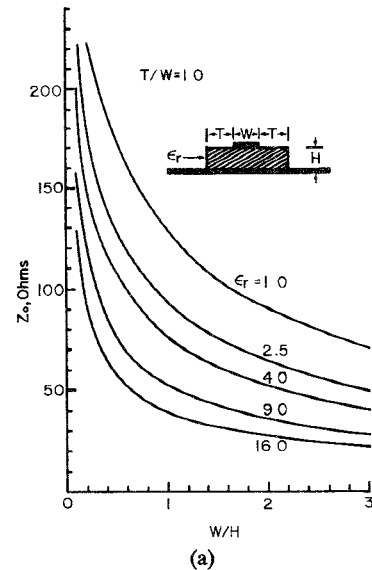


(b)

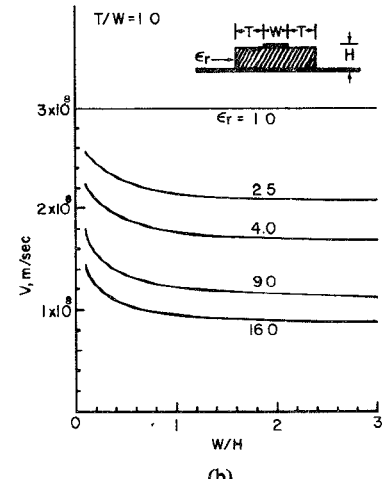
Fig. 4. (a) Characteristic impedance of microstrip for $T/W=2.0$. (b) Velocity of propagation on microstrip for $T/W=2.0$.

and near the strip. It is a direct result of this small magnitude in conjunction with distance between regions that the truncation does not greatly influence the propagation characteristics.

Computations reveal that as T is increased to large values for a fixed W/H ratio, the magnitude of charge density in the truncation region decreases, thereby reducing its contribution to (and effect on) the fields near the source strips; however, for small T/W ratios this region does contribute significantly to the fields structure which results in changes in the propagation characteristics of the microstrip transmission line. The actual effect of symmetrical truncation of microstrip transmission lines is shown in Figs. 4-7 where computed values of characteristic impedance and velocity of propagation are plotted for several truncation width ratios T/W and relative dielectric constants as a function of W/H . A comparison of the data of Figs. 4-7 and the infinite-width data³ of Bryant



(a)



(b)

Fig. 5. (a) Characteristic impedance of microstrip for $T/W=1.0$. (b) Velocity of propagation on microstrip for $T/W=1.0$.

and Weiss [3] indicates that microstrip transmission line can be truncated at $T/W=1$ in most cases without significantly affecting either the characteristic impedance or the velocity of propagation. This property is not entirely unexpected; however, after the numerical results were obtained, it was surprising to find how close the truncation could be made without changing the line characteristics.

Another problem of the same class is nonsymmetrical truncation of the dielectric structure as it is related to the question, "How close to the edge of dielectric can a strip be placed without altering the propagation characteristics from that of the infinite-width model?" A similar numerical procedure has been developed and programmed to compute the characteristic impedance for this nonsymmetrical electrostatic problem, and results of this computation are presented in Fig. 8 for one case along with data for the corresponding symmetrical truncation. From a practical point of view, it would be expected that propagation would not be influenced as much by symmetrical

³For example, see dotted lines in Fig. 4.

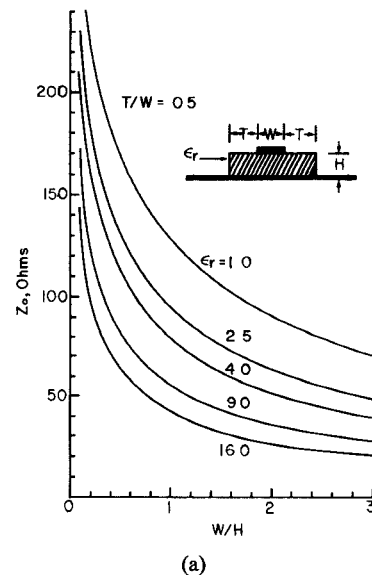


Fig. 6. (a) Characteristic impedance of microstrip for $T/W = 0.5$. (b) Velocity of propagation on microstrip for $T/W = 0.5$.

truncation since less dielectric is removed. This is indeed the case as can be seen from a comparison of the solid and dotted lines in Fig. 8.

CONCLUSIONS

It has been shown that the propagation characteristics of symmetrical and nonsymmetrical truncated microstrip transmission lines⁴ remain essentially unchanged from those of the infinite-width line for $T/W > 1$, although an appreciable variation occurs for $T/W < 0.5$. The detailed dependence of truncation on the choice of dielectric material and the choice of W/H ratios may be obtained from Figs. 4-7. In addition, the parameter study of the propagation characteristics of Figs. 4-7 provides informa-

⁴These models represent practical cases of microstrip line with finite-width dielectric and metal clad mounted on a metal support block. TDR measurements indicate that for small T/W ratios positive contact of the support block and metal clad must be maintained to obtain characteristics presented in this parameter study.

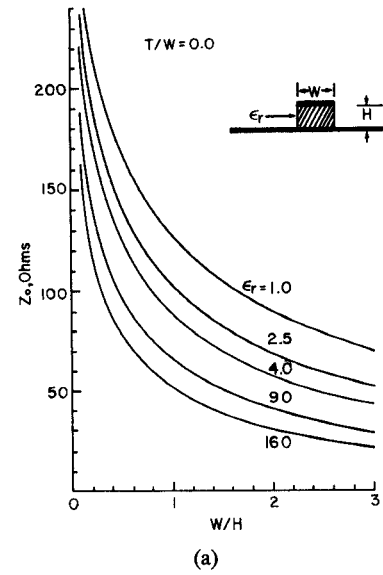


Fig. 7. (a) Characteristic impedance of microstrip for $T/W = 0.0$. (b) Velocity of propagation on microstrip for $T/W = 0.0$.

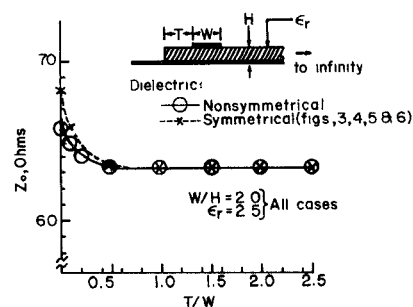


Fig. 8. Characteristic impedance for nonsymmetrical microstrip line (solid line).

tion for the design of impedance transformers using tapered-dielectric transmission lines with fixed W/H ratios.

REFERENCES

- [1] S. March, "Microwave micromini bibliography," *Microwaves*, vol. 8, no. 12, pp. 59-64, Dec. 1969.
- [2] —, "Microwave micromini bibliography (cont'd)," *Microwaves*,

vol. 9, no. 1, pp. 53-56, 122, 124, Jan. 1970.

[3] T. G. Bryant and J. A. Weiss, "Parameters of microstrip transmission lines and of coupled pairs of microstrip lines," *IEEE Trans. Microwave Theory Tech.*, vol. MTT-16, pp. 1021-1027, Dec. 1968.

[4] A. Farrar and A. T. Adams, "Characteristics impedance of microstrip by the method of moments," *IEEE Trans. Microwave Theory Tech.*, vol. MTT-18, pp. 65-66, Jan. 1970.

[5] P. Silvester, "TEM wave properties of microstrip transmission lines," *Proc. IEE (London)*, vol. 115, pp. 43-48, Jan. 1968.

[6] A. Farrar and A. T. Adams, "Computation of lumped microstrip capacitances by matrix methods-rectangular sections and end effect," *IEEE Trans. Microwave Theory Tech.*, vol. MTT-19, pp. 495-497, May 1971.

[7] T. Itoh and R. Mittra, "A new method for calculating the capacitance of a circular disk for microwave integrated circuits," *IEEE Trans. Microwave Theory Tech.*, vol. MTT-21, pp. 431, 432, June 1973.

[8] A. Farrar and A. T. Adams, "Method of moments applications volume VI—Matrix methods for static microstrip," Rome Air Development Center, Rep. RADC-TR-73-217, vol. VI, Feb. 1975.

[9] R. F. Harrington, *Field Computation by Moment Methods*. New York: Macmillan, 1968.

[10] R. F. Harrington and K. Pontoppidan, "Computation of Laplacian potentials by an equivalent source method," *Proc. IEE*, vol. 116, no. 10, pp. 1715-1720, Oct. 1969.

[11] A. T. Adams and J. R. Mautz, "Computer solution of electrostatic problems by matrix inversion," in *Proc. Nat. Electronics Conf.*, vol. 25, pp. 198-201, Dec. 1969.

[12] C. E. Smith, "A coupled integral equation solution for microstrip transmission lines," in *IEEE G-MTT Microwave Symp. Dig.*, pp. 284-286, June 1973.

[13] R. F. Harrington, *Time-Harmonic Electromagnetic Fields*. New York: McGraw-Hill, 1961.

[14] R. S. Chang, "A numerical solution technique for the truncated microstrip transmission line," M.S. thesis, University of Mississippi, University, Aug. 1975.

Coupled Microstrip Disk Resonators

NIKOLAOS K. UZUNOGLU and P. KATECHI

Abstract—The coupling between microstrip disk resonators is investigated analytically and experimentally. The interaction between the printed disks is modeled by a gap capacitance, which is computed by solving the corresponding electrostatic problem. An integral equation is used to determine the nonsymmetric charge distribution on the disk resonators. Numerical results are presented for several cases. For a specific case the prediction of the theory is compared with the experiment.

I. INTRODUCTION

THE GAP CAPACITANCE for microstrip printed circuits [1], [2] is investigated by several authors, where mostly linear edge shapes are treated. In this article the coupling between printed disk resonators is considered.

The geometry of the problem is defined in Fig. 1. The coupled disk resonators are printed on a grounded dielectric substrate. The substrate thickness is H with a relative dielectric constant ϵ_r . Also a second perfect conductor-ground plane is assumed at $z = B$. The coupling between the two resonators is assumed to be mainly due to the fringing effects of the electric fields; and, as a result, the coupling between the two disks can be modeled by a gap capacitance C_g . In Section II a method for computing C_g is developed. The method is based on using the cylindrical coordinates in conjunction with Galerkin technique. The

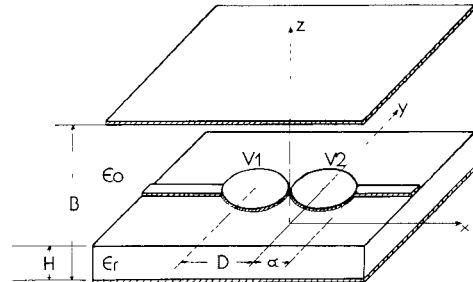


Fig. 1. Coupled resonator geometry.

resonance frequencies for disk resonators can be computed by assuming infinite magnetic conductivity resonators walls [3]. The behavior of coupled resonators can be predicted by considering an equivalent circuit around each resonance frequency.

Assuming the disks to be raised at $V_1 = 1/2$ and $V_2 = -1/2$ V the total charge on each disk will be

$$Q(D) = C_g(D) + (1/2)C \quad (1)$$

where C is the self capacitance of each disk. For very large D values

$$\lim_{D \rightarrow +\infty} Q(D) = (1/2)C$$

so the gap capacitance will be

$$C_g(D) = Q(D) - \lim_{D \rightarrow +\infty} Q(D). \quad (2)$$

Manuscript received August 28, 1978; revised April 3, 1979. This project was supported by the NTUA Research Council.

The authors are with the Department of Electrical Engineering, National Technical University of Athens, Athens, 147, Greece.